

White-Box Evaluation of Fingerprint Matchers

Steven A. Grosz, *Member, IEEE*, Joshua J. Engelsma
Nicholas G. Paulter Jr., *Fellow, IEEE*, and Anil K. Jain, *Life Fellow, IEEE*,

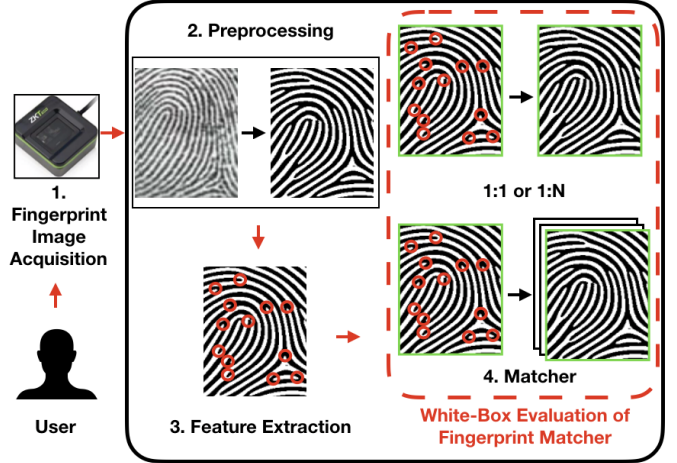
Abstract—Prevailing evaluations of fingerprint recognition systems have been performed as end-to-end black-box tests of fingerprint identification or verification accuracy. However, performance of the end-to-end system is subject to errors arising in any of the constituent modules, including: fingerprint reader, preprocessing, feature extraction, and matching. While a few studies have conducted white-box testing of the fingerprint reader and feature extraction modules of fingerprint recognition systems, little work has been devoted towards white-box evaluations of the fingerprint matching sub-module. We report results of a controlled, white-box evaluation of one open-source and two commercial-off-the-shelf (COTS) state-of-the-art minutiae-based matchers in terms of their robustness against controlled perturbations (random noise, and non-linear distortions) introduced into the input minutiae feature sets. Experiments were conducted on 10,000 synthetically generated fingerprints. Our white-box evaluations show performance comparisons between different minutiae-based matchers in the presence of various perturbations and non-linear distortion, which were not previously shown with black-box tests. Furthermore, our white-box evaluations reveal that the performance of fingerprint minutiae matchers are more susceptible to non-linear distortion and missing minutiae than spurious minutiae and small positional displacements of the minutiae locations. The measurement uncertainty in fingerprint matching is also developed.

Index Terms—Fingerprint recognition systems, minutiae matching module, white-box evaluation, non-linear distortion, uncertainty analysis

I. INTRODUCTION

FINGERPRINT recognition for person identification and authentication is one of the long-standing and most reliable biometric recognition techniques. The use of fingerprints has seen a tremendous growth over the past 20 years due to their purported uniqueness, permanence, universality, and ease of collection [1]. With their first use in the forensics community in the early 1900s, fingerprint recognition systems have now permeated into a myriad of applications, including finance, healthcare, mobile phones, and border crossings [1]. As fingerprint recognition technology continues to see widespread adoption, the need to understand and validate system recognition accuracy and robustness is paramount. This necessitates a sound, repeatable, controlled evaluation procedure of the various sub-modules of fingerprint recognition systems, including: image acquisition, preprocessing, feature extraction, and matching (see Figure 1).

Current methods for evaluating automated fingerprint identification systems (AFIS) consist, almost entirely, of end-to-



Black-Box Evaluation of Fingerprint Recognition System

Fig. 1: Pipeline of a typical fingerprint recognition system: (1) fingerprint acquisition, (2) preprocessing, (3) feature extraction, and (4) matching. While existing evaluations of recognition systems primarily consist of an end-to-end black-box evaluation (i.e. all 4 modules simultaneously), we propose an independent, white-box evaluation of the matching module.

end black-box testing¹. In particular, the verification accuracy (1:1 match) and the identification accuracy (1:N search) are reported after (i) collecting fingerprints from a number of subjects, (ii) obtaining similarity scores from the fingerprints by propagating them through all the four modules of fingerprint recognition system, and (iii) applying a decision threshold on the similarity scores to make an identity determination. For example, the National Institute of Standards and Technology (NIST) conducts fingerprint vendor technology evaluations (FpVTE) [8] and the University of Bologna conducts fingerprint verification competitions (FVC) [9], [10] to evaluate fingerprint recognition systems on their operational performance, as measured in terms of computational requirements and recognition accuracy.

Black-box evaluations are valuable in that they allow for overall comparisons between state-of-the-art recognition systems in terms of performance from the perspective of an end-user. This allows an end-user to select the fingerprint recognition system that performs the best in their specific application domain. However, this black-box testing approach is limited in that it does not provide either the designer or the end user any information on which sub-module of the AFIS is actually causing recognition failures.

To address this limitation inherent to black-box testing, we aim to build upon recent studies that performed white-box

J. J. Engelsma, S. A. Grosz, and A. K. Jain are with the Department of Computer Science and Engineering, Michigan State University, East Lansing, MI, 48824 E-mail: {engelsm7, groszste, jain}@msu.edu

N. G. Paulter Jr. is with the National Institute of Standards and Technology (NIST), Gaithersburg, Maryland 20899 Email: paulter@nist.gov

¹White-box testing evaluates the internal sub-components of a system, whereas black-box testing focuses on testing the end-to-end system using system inputs and outputs [7].

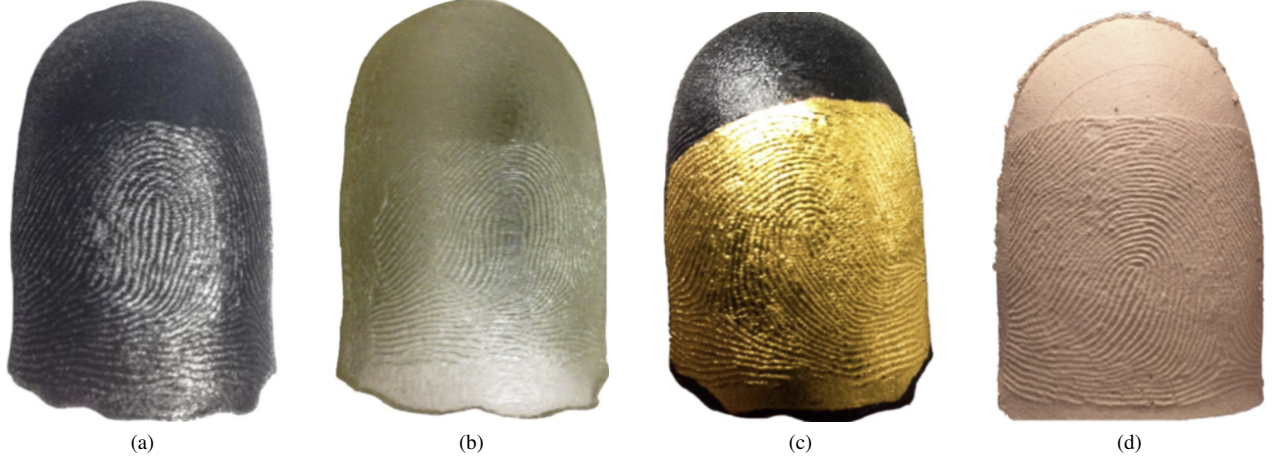


Fig. 2: 3D fingerprint targets. (a) printed using TangoBlackPlus FLX980 [2], (b) printed using TangoPlus FLX 930 and used in construction of whole hand targets proposed in [3], (c) printed using TangoBlackPlus FLX980 and then sputter coated with 30 nm titanium + 300 nm of gold [4], and (d) universal target produced using a mixture of conductive PDMS, silicone thinner, and Pantone 488C color pigment [5] Figure reproduced from [5].



Fig. 3: Two different levels of additive noise and motion blur. (a) reference fingerprint, (b) noise level 1, (c) noise level 2, (d) motion blur level 1, and (e) motion blur level 2. Figure adapted from [6].

evaluations of individual modules of fingerprint recognition systems [2], [3], [4], [5], [6]. To date, prior work in white-box evaluations of AFIS have primarily targeted the fingerprint reader and feature extraction modules. In particular, Arora et al. designed and fabricated 3D fingerprint targets with similar hardness and elasticity to the human skin to assess the image capture fidelity of different fingerprint readers [2] (Fig. 2 (a)). Arora et al. also designed 3D whole-hand targets to evaluate slap and contactless fingerprint readers [3] (Fig. 2 (b)) and 3D gold-finger targets for evaluating capacitive readers [4] (Fig. 2 (c)). Engelsma et al. built upon the work of Arora et al. by

designing a single target (universal target) which could be used to evaluate all major types of fingerprint readers commercially available (capacitive, contact-optical, contactless-optical, and ultrasound) [5] (Fig. 2 (d)). Additionally, Chugh et al. conducted white-box studies of minutiae extractors by studying their robustness to controlled levels of noise and motion blur (3) [6]. The additive noise used in Chugh et al. was modeled in Novetta’s biosynthetic software [11] to simulate (i) structural deformations (scars, holes, and pressure variation), (ii) ridge noise, and (iii) finger dryness. A few studies have also attempted a white-box evaluation of latent fingerprint examiners, by quantifying discrepancies between manual markups made by human experts [12], [13], [14]. Despite these efforts, to the best of our knowledge, there has been no attempt to conduct a white-box evaluation of the matcher module of automated fingerprint recognition systems.

Given the lack of a standard, white-box evaluation of fingerprint minutiae-matchers in the literature, we propose a rigorous, repeatable white-box evaluation protocol for state-of-the-art minutiae based matchers. This protocol consists of the following steps:

- 1) Perturb a “ground-truth” minutiae-set (provided by the synthetic fingerprint generator, SFinge [15]) by (i) random translation and rotation shifts to the individual minutiae, (ii) random minutiae additions (spurious minutiae) and minutiae deletions (missing-minutiae), (iii) combined random translation/rotation shifts and addition/removal of minutiae, and (iv) non-linear distortion via the thin-plate spline model.
- 2) Compare unperturbed “ground-truth” templates and the perturbed templates to obtain genuine and imposter similarity score distributions associated with each perturbation.
- 3) Compute an uncertainty score for each matcher due to the perturbation techniques.

Our analysis aims to measure the robustness of various minutiae-based matchers against the induced minutiae perturbations and reveal insights into the strengths of the minutiae-

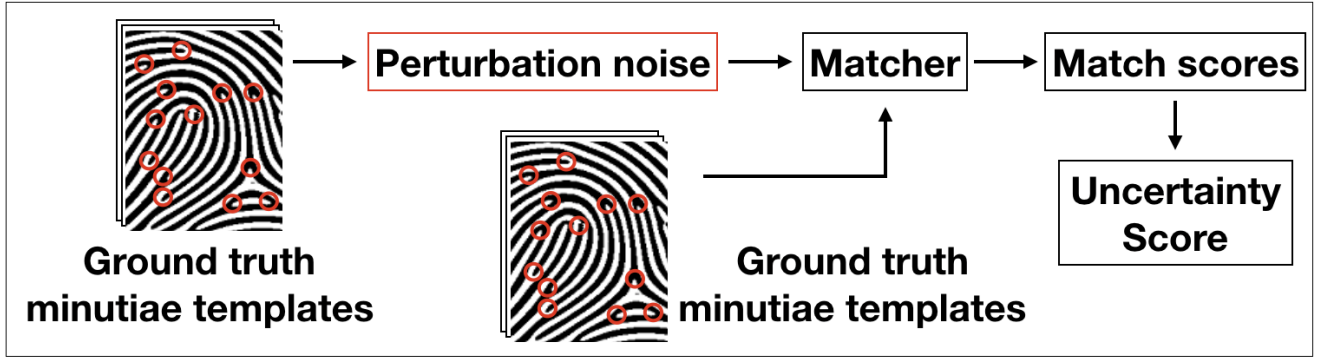


Fig. 4: Overview of the white-box testing of a minutiae-matcher. Input minutiae sets are perturbed by random positional perturbations and non-linear distortions. The perturbed minutiae sets are then matched to the unmodified templates to generate similarity scores. Lastly, a measurement uncertainty associated with each type of perturbation is computed, which indicates a measure of robustness to that type of perturbation.

based matchers, not previously revealed with black-box testing, through the development of measurement uncertainty. More concretely, the contributions of this research are as follows:

- 1) A robust white-box evaluation protocol for the fingerprint matching module. This evaluation augments previous studies on white-box evaluations of the fingerprint reader [2][3][4] and feature extractor modules [6].
- 2) An analysis on the effects of random positional perturbations and non-linear distortion on minutiae-matcher performance.
- 3) Benchmarking three state-of-the-art minutiae-matchers in accordance with our proposed protocol: (i) an open source matcher (SourceAFIS) [16] and (ii) two COTS matchers (Verfinger and Innovatrics)².
- 4) Establishment of rigorous measurement uncertainty.

II. EVALUATION PROCEDURE

The primary objective of our white-box evaluation protocol is to perform a measurement uncertainty analysis [17] of minutiae-based matchers. Uncertainty analysis provides a measure for “goodness” of a test result and allows one to assign credibility limits to the accuracy of a reported value [17]. An uncertainty analysis of the matcher module reveals its contribution to the overall accuracy of the encompassing AFIS. More specifically, this analysis provides a measure on the performance of the matcher in comparing ground-truth minutiae templates with templates perturbed with various positional variations and distortion. An overview of the analysis is shown in Figure 4.

We conduct two main experiments in our white-box evaluation of fingerprint minutiae matchers. First, we perform an uncertainty analysis resulting from realistic amounts of perturbation and non-linear distortion that one could reasonably expect to encounter in an operational scenario. The specific perturbation parameters were chosen to reflect results from previous research on minutiae feature extractors in Chugh et al. [6]. In an additional experiment, we evaluate recognition performance of each minutiae matcher on increasing levels of perturbation and distortion.

²these two matchers are among the highest performing matchers in the NIST FpVTE

A. Data Set for Experiments

The first step to perform an uncertainty analysis of a minutiae-based matcher is to obtain ground-truth minutiae-sets. We obtain the ground-truth minutiae-sets from fingerprints synthetically generated using SFinGe [15]. The process to generate a synthetic fingerprint in SFinGe is as follows (steps 1-3 are used to generate the fingerprint pattern and ground-truth minutiae locations and steps 4-10 are responsible for producing realistic-looking fingerprint impressions):

- 1) Specify the type (thumb, index, etc.) and shape of the fingerprint pattern.
- 2) Select the fingerprint class (arch, left loop, right loop, whorl, tented arch) and position of singularities (core, delta).
- 3) Select the number of seeds and ridge density value.
- 4) Select the number of permanent scratches in ridge-valley impression.
- 5) Adjust the finger contact region by applying a displacement up, down, left, or right.
- 6) Increase or decrease the ridge line thickness for varying levels of pressure/dryness.
- 7) Choose the amount of distortion to add.
- 8) Select the level of additive noise³ for a more realistic looking impression.
- 9) Choose any level of rotation and translation to the fingerprint image.
- 10) Select a background (none, capacitive, optical, etc.) and amount of contrast for the synthetic print.

We have generated 5,000 unique “master”⁴ reference fingerprints, each of which is synthesized to produce two synthetic impressions (Fig. 5). Thus, a total of 10,000 fingerprints are used (5,000 unique fingers, 2 impressions per finger). For each of the 5,000 fingerprints that SFinGe generates, a ground truth minutiae feature set is also output. It is these minutiae sets that are fed as input to the fingerprint matchers for evaluation.

We utilize synthetic fingerprints because they provide reliable, consistent, ground-truth minutiae-sets. Obtaining ground-

³This additive noise was not the subject of this research, but merely added to make the impressions more realistic.

⁴Here master print refers to the original binary print generated by SFinGe prior to any distortion and/or noise that is introduced to produce realistic looking fingerprint images.

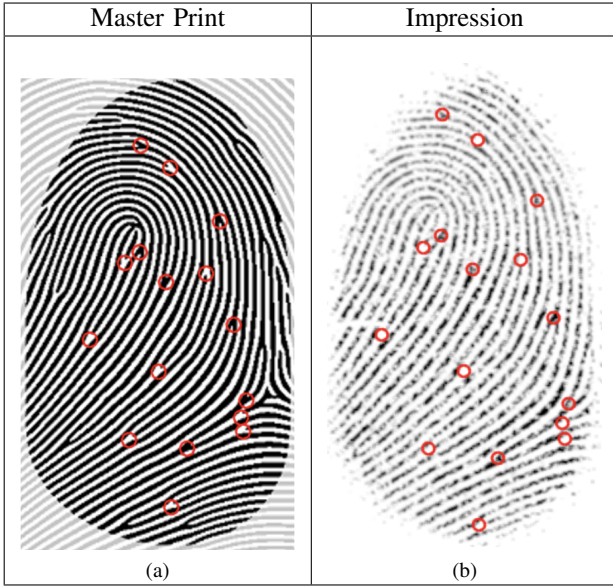


Fig. 5: Example fingerprint images obtained from SFinGe synthetic fingerprint generator. (a) A master print with ground truth minutiae points; (b) a realistic impression of the same fingerprint, derived from the master print. Notice that the ground truth minutiae locations are preserved after addition of noise to the fingerprint image.

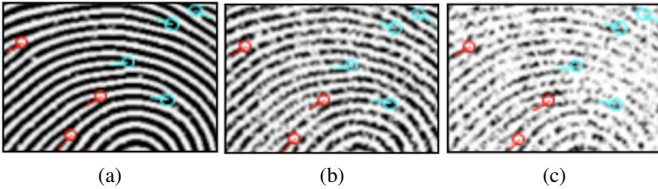


Fig. 6: Illustration of ground truth minutiae annotations in a portion of a fingerprint image for three levels of image quality obtained with SFinGe synthetic fingerprint generator. (a) Master fingerprint with ground truth. (b) Slightly noisy fingerprint with overlaid ground truth obtained from the master print. (c) Highly noise-degraded fingerprint, yet with accurate ground truth minutiae annotations.

truth minutiae-sets from an operational fingerprint dataset necessitates the use of minutiae sets output by the fingerprint recognition system's feature extractor on *noisy* fingerprints, such as those shown in Fig. 6 (b) and (c). Different feature extractors will output different ground truth minutiae-sets, and likely bias the performance of the matcher towards the feature extractor used. This defeats the paramount goal of a white-box evaluation of the matcher, which is to evaluate the performance of the matcher independent of the feature extractor (or other sub-modules) used.

Conversely, minutiae sets can be extracted easily and without ambiguities from synthetic fingerprints since the minutiae are extracted from master-prints (Fig. 6 (a)) (binary synthetic images which have not been subjected to noise and distortion). Figure 6 shows that the preservation of minutiae extracted from the binary master-print through increasing levels of image degradation in the generation of realistic fingerprint images. Thus, synthetic prints can be used to obtain reliable, consistent minutiae feature sets that can be used as input to any matcher to measure uncertainty in matching.

B. Perturbation Techniques

Given a ground truth minutiae feature set $\{(x_1, y_1, \theta_1), \dots, (x_n, y_n, \theta_n)\}$, the next step in the uncertainty analysis is the perturbation of the individual ground-truth minutiae by two types of perturbations: randomly generated positional perturbation and non-linear distortion. In particular, the minutiae perturbation techniques applied are: (i) random positional (translational and rotational) shifts, (ii) random addition and removal (spurious and missing) of minutiae, (iii) combined random positional shifts and addition/removal of minutiae, and (iv) non-linear distortion (thin-plate spline distortion model). The random perturbations are each applied independently to individual minutiae and again in aggregate to give both a granular and overall evaluation of the robustness of the minutiae-based matcher to the various types of perturbation. These perturbation techniques are illustrated in Figure 7.

1) *Translational and Rotational Shifts*: It was shown in [6] that different fingerprint minutiae extractors will provide slightly different x , y , and θ values. Therefore, the first perturbation technique involves random translation and rotation applied to the x , y , and θ of each minutiae. In a study on fingerprint uniqueness [18], Zhu et al. determined that the distribution of minutiae positions can be appropriately modeled by a multi-variate Gaussian distribution. Therefore, in keeping with established research, we use Gaussian distribution models to distribute random noise to the positions and orientations of the fingerprint minutiae.

The mean, μ , and standard deviation, σ , parameters of the Gaussian distributed translational (μ_p and σ_p) and rotational (μ_o and σ_o) variations are taken from the literature [6]. In [6], a white-box evaluation of fingerprint feature extractors was performed on 3,458 real fingerprint images aggregated from five different public domain databases: FVC 2002 (DB1A and DB3A), FVC 2004 (DB1A and DB3A), and the NIST SD27 rolled prints database. In particular, the average translation and rotation errors were obtained as the distance between the minutiae locations provided by the automated feature extractor and the manually annotated ground truth minutiae locations. These values were binned (into 5 bins)⁵ based upon the NFIQ 2.0 [19] quality metric associated with the input fingerprint to the feature extractor. Therefore, we take the weighted average of these values across each bin (weights based on number of images in the bin) as the mean and standard deviation for our models of Gaussian distributed perturbation. The values (in pixels) obtained for μ_p and σ_p of the translational translation are 4.048 and 0.688, respectively. The values (in radians) obtained for μ_o and σ_o of the rotational perturbation are 0.130 and 0.071, respectively. The procedure for applying this type of perturbation is described in Algorithm 1.

2) *Removal of Genuine and Addition of Spurious Minutiae*: A commonly occurring variation in minutiae feature sets is the number of minutiae points identified in a fingerprint image by various feature extractors. The number of detected minutiae points can either be lower than ground-truth (due to missed

⁵The values assigned by the NFIQ 2.0 quality metric range from 0 to 100 and the ranges of the individual bins are [0, 20], [21, 40], [41, 60], [61, 80], and [81, 100].

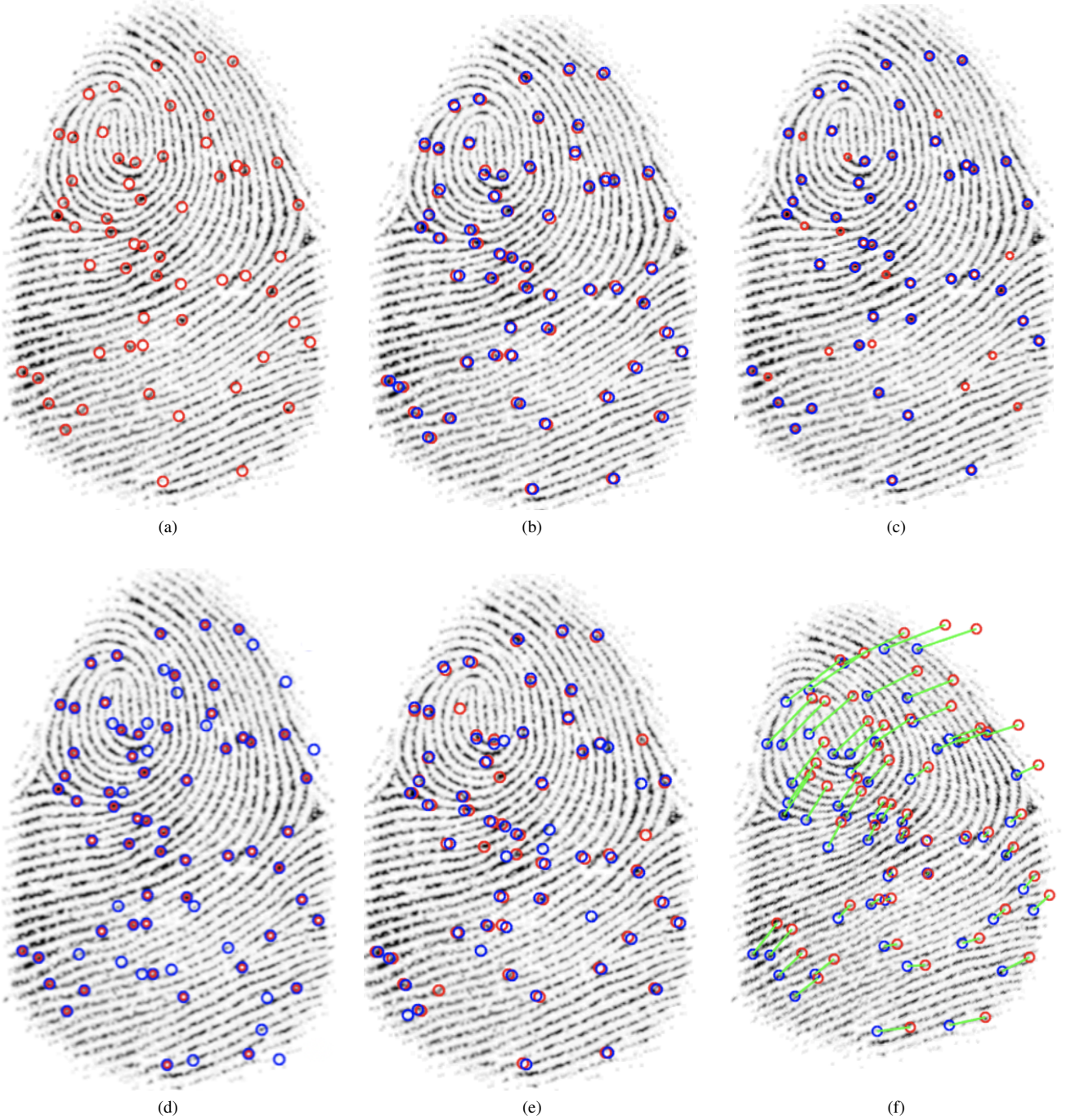


Fig. 7: Illustration of the various minutiae perturbation techniques. For each image, the red circles denote the original minutiae locations and the blue circles designate the minutiae locations following the perturbations. (a) The original, ground truth minutiae locations, (b) random positional shifts of x , y , and θ , (c) removal of random minutiae points, (d) addition of random minutiae points, (e) combined positional and missing/spurious minutiae, and (f) non-linear distortion of minutiae pattern.

detections) or higher than ground-truth (false detections). Therefore, our evaluation protocol takes into account the effects of spurious and missing minutiae on minutiae-based matchers.

Similar to the previously discussed positional perturbation technique, the distributions of missing minutiae and spurious minutiae are modeled by Gaussian distributions whose parameters are set as the true expected value and variance of the differences observed in the output of various state-of-the-

art feature extractors [6]. As in [6], the mean and standard deviation values are reported as a ratio of the number of missed minutiae to the total number of ground truth minutiae in the fingerprint image. The mean and standard deviation values for the spurious minutiae (taken from [6]) are 0.523 and 0.349, respectively, whereas those for the missing minutiae are 0.209 and 0.106, respectively.

3) *Combined Positional Perturbation with Missing and Spurious Minutiae*: This perturbation technique involves ag-



Input Fingerprint

Distorted Fingerprints

Fig. 8: Applying non-linear distortion fields (obtained from a statistical model [20]) to an input fingerprint. Note, we show the fingerprint images here to illustrate the effects of the non-linear distortion on fingerprint images. However, in the experiments, we directly apply the distortion field to ground truth minutiae points provided by SFinge, eliminating the need of a feature extractor for this white-box evaluation of the matcher.

Algorithm 1 Translation and Rotation Perturbation

Input: $x, y, \theta, \mu_o, \sigma_o, \mu_p, \sigma_p$

Output: x', y', θ'

- Generate $d\theta$ from μ_o and σ_o of rotational distribution:
 - 1: $d\theta = \text{rand.normal}(\mu_o, \sigma_o)$
 - Calculate new θ' :
 - 2: $\theta' = \text{mod}(\theta + d\theta, 2\pi)$
 - Generate dr from μ_p and σ_p of translational distribution:
 - 3: $dr = \text{rand.normal}(\mu_p, \sigma_p)$
 - Calculate dx and dy from θ' and dr :
 - 4: $dx = dr \cos \theta'$
 - 5: $dy = dr \sin \theta'$
 - Calculate x' and y' :
 - 6: $x' = x + dx$
 - 7: $y' = y + dy$
-

gregating the previously discussed techniques into one. This technique is intended to show the combined effects of the positional perturbations and the presence of missing and spurious minutiae, which is more representative of what a matching module might reasonably encounter in an operational setting.

First, we delete some minutiae points from the input minutiae feature set as described previously, followed by insertion of some spurious minutiae. Lastly, we apply the translation and rotation perturbations. The missing minutiae perturbation technique is first applied so that none of the added spurious minutiae are deleted.

4) *Non-Linear Distortion Model*: The final perturbation technique applied to the input minutiae feature set is that of an applied non-linear distortion model proposed by Si et al. in [20]. We chose to apply a non-linear distortion model (learned from actual distorted fingerprints) as a perturbation to the minutiae points since much of the perturbation of the minutiae points in an operational scenario will be from distortion introduced by the elastic friction ridge pattern on the

human fingertip. Furthermore, it is important to evaluate the robustness of a minutiae-matcher against non-linear distortion since it has been shown that hackers can obfuscate their own identity by intentionally introducing a heavy distortion to their fingerprints during the fingerprint acquisition process [20].

The non-linear distortion model proposed in [20] is formulated and trained as follows. (i) A database of 320 distorted fingerprint videos was acquired. (ii) The minutiae are extracted from the first and last frame of the video sequence. (iii) Correspondences are computed between the minutiae from the first frame and the minutiae in the final, distorted fingerprint frame. (iv) The corresponding minutiae points are used to estimate a distortion field d_i (grid) using the Thin-Plate-Spline (TPS) model [21]. (v) Each distortion field d_i is flattened into a vector and used to compute a mean distortion field \bar{d} . Subsequently, a covariance matrix D is constructed. (vi) From the covariance matrix, Principle Component Analysis (PCA) is used as a statistical model to capture the variance of the training distortion fields. Therefore, a new distortion field d can be generated from a subset of t eigenvectors in accordance with Equation 1:

$$d \approx \bar{d} \sum_{i=1}^{i=t} c_i \sqrt{\lambda_i} e_i \quad (1)$$

where c_i are the coefficients of the eigenvectors e_i .

In our work, we select the coefficients c_i of two eigenvectors (with the largest two eigenvalues) to generate new distortion fields from a normal distribution with mean of zero and standard deviation of $2/3$. These parameters were chosen to be consistent with the work of [20], where the authors chose coefficients uniformly in the range of $[-2, 2]$. We chose to select values from a normal distribution from roughly the same range to avoid biasing the random selection. These randomly generated non-linear distortion fields are then applied to an unperturbed minutiae set. Note that we do not apply the distortion field to the fingerprint image (as was done in [20]). Instead, we directly apply the distortion field to the minutiae points. This prevents us from having to use a feature extractor to locate the minutiae points in a distorted image (which would taint the white-box matcher evaluation). Examples of

fingerprints before and after applying the non-linear distortion model are shown in Figure 8.

C. Uncertainty Analysis Procedure

We evaluate matcher performance on each of the given perturbation techniques. Similarity scores between the original fingerprint template and the perturbed template are computed. From these scores, a total uncertainty is assigned to each fingerprint matcher chosen for the study. The step-by-step procedure used to calculate the uncertainty of a fingerprint matcher to controlled perturbations (random positional perturbations and non-linear distortions) introduced into the input minutiae feature sets is as follows:

- 1) Generate $M = 10,000$ unique $A_{ref,k}$ as reference fingerprint impressions from the SFinGe synthetic fingerprint generator, $1 \leq k \leq M$.
- 2) Obtain M unique minutiae feature sets, $S_{ref,k}$, from each $A_{ref,k}$.
- 3) For each reference minutiae set, $S_{ref,k}$, we synthesize $N = 100$ different perturbed minutiae sets, $S'_{test,k,n}$, $1 \leq n \leq N$.
- 4) Generate genuine similarity scores, $s_{k,n}$, between $S_{ref,k}$ and each $S'_{test,k,n}$ using the public-domain minutiae matcher [16], COTS-A, and COTS-B.
- 5) Normalize the scores, $s_{k,n}$, to be in the range of $[0,1]$.
- 6) Compute the average, μ_k , of the $s_{k,n}$ scores using Equation 2:

$$\mu_k = \frac{1}{N} \sum_{n=1}^N (s_{k,n}) \quad (2)$$

- 7) Compute the standard uncertainty, u_k , of A_k using Equation 3:

$$u_k = \sqrt{\frac{1}{N} \sum_{n=1}^N (\mu_k - s_{k,n})^2} \quad (3)$$

- 8) Repeat steps 1-7 for each reference feature set, obtaining a u_k for each $S_{ref,k}$.
- 9) Compute the total uncertainty, $u_{matcher}$, for the matcher using Equation 4

$$u_{matcher} = \sqrt{\frac{1}{M} \sum_{k=1}^M u_k^2} \quad (4)$$

This uncertainty calculation uses the Monte Carlo method [22] for estimating uncertainties. It demonstrates the sensitivity of a matcher to perturbations of its inputs. To augment the findings of the uncertainty calculation, we also compute genuine and imposter similarity scores between multiple impressions of the same finger, where one template has been perturbed. In other words, we obtain one distribution of similarity scores from each reference template and its corresponding perturbed templates to calculate the uncertainty resulting from the perturbations, and another distribution from corresponding (unperturbed, perturbed) impression pairs to

evaluate the effects of the perturbation on recognition accuracy between matching fingerprint impressions following the perturbations.

D. Recognition Accuracy vs. Perturbation Procedure

Here we discuss the experimental design for evaluating the recognition accuracy of the minutiae-based matchers on increasing levels of perturbation. For this experiment, we select 2,000 fingerprints and their corresponding pair of synthetic impressions from our synthetic database (4,000 total synthetic fingerprint impressions). For each pair, we perturb one of the fingerprint impressions with each of the perturbation techniques and calculate the genuine similarity scores between the perturbed and unperturbed impressions. Thus, for each perturbation technique, we calculate 2,000 genuine similarity scores. Additionally, we randomly select 50,000 non-corresponding perturbed, non-perturbed impression pairs to calculate 50,000 imposter similarity scores. Then, we calculate the true acceptance rate (TAR) at a constant false acceptance rate (FAR) of 0.01%. We run eight iterations of increasing perturbation of each type and calculate the TAR at each iteration to track the recognition accuracy vs. perturbation amount (Table I). For each of the five perturbation techniques, we calculate 2,000 genuine scores and 50,000 imposter scores at each of the eight iterations.

III. EXPERIMENTAL RESULTS

Using the synthetic fingerprint data set and perturbations defined previously, we evaluate the effects of the various perturbation techniques on the performance of each minutiae matcher in the study. We examine the distributions of genuine and imposter similarity scores before and after the perturbations and calculate the uncertainty observed in each of the minutiae matchers. Histograms of the genuine and imposter similarity distributions for each minutiae matcher following the realistic perturbations are shown in Figure 9 and the normalized mean and standard deviation of each distribution is shown in Table II. The measurement uncertainty of matching associated with each type of perturbation are shown in Table III. Finally, matcher recognition accuracy vs. increasing levels of perturbation and distortion are shown in Figure 10.

A. Effect of Random Perturbations

To analyze the effects of random perturbation (position shifts and addition and removal of minutiae points), we compare the genuine and imposter similarity scores of each minutiae matcher before and after the applied perturbations. The initial step in the analysis involves computing genuine similarity scores on the minutiae feature sets between the two impressions (prior to any perturbations) of each fingerprint in the data set. More concretely, we have 5,000 unique fingerprint templates with two synthetic impressions each denoted by $A_{k,n}$, $1 \leq k \leq 5000$ and $1 \leq n \leq 2$. We obtain minutiae feature sets, $S_{k,n}$, and compute the genuine similarity score between each pair of genuine impressions denoted by $s_{k,genuine}$. Next, we perform the positional and

TABLE I: Increasing Perturbation Parameters

Iteration Number	1	2	3	4	5	6	7	8
Positional Displacement (Pixels)	5	10	15	20	25	30	35	40
Missing Minutiae (Missing Minutiae / Ground Truth)	0.20	0.40	0.60	0.80	0.85	0.90	0.95	0.99
Spurious Minutiae (Spurious Minutiae / Ground Truth)	0.5	1.0	1.5	2.0	max	max	max	max
Combined Random Perturbation (Pixel Displacement, Missing Minutiae / Ground Truth, Spurious Minutiae / Ground Truth)	5, 0.20, 0.5	10, 0.40, 1.0	15, 0.60, 2.0	20, 0.80, 1.5	25, 0.85, max	30, 0.90, max	35, 0.95, max	40, 0.99, max
Non-Linear Distortion (Std. Dev.)	0.5	1.0	1.5	2.0	2.5	3.0	3.5	4.0

Max refers to the maximum number of minutiae points as allowed by the ISO minutiae template standard, which is 255 minutiae points.

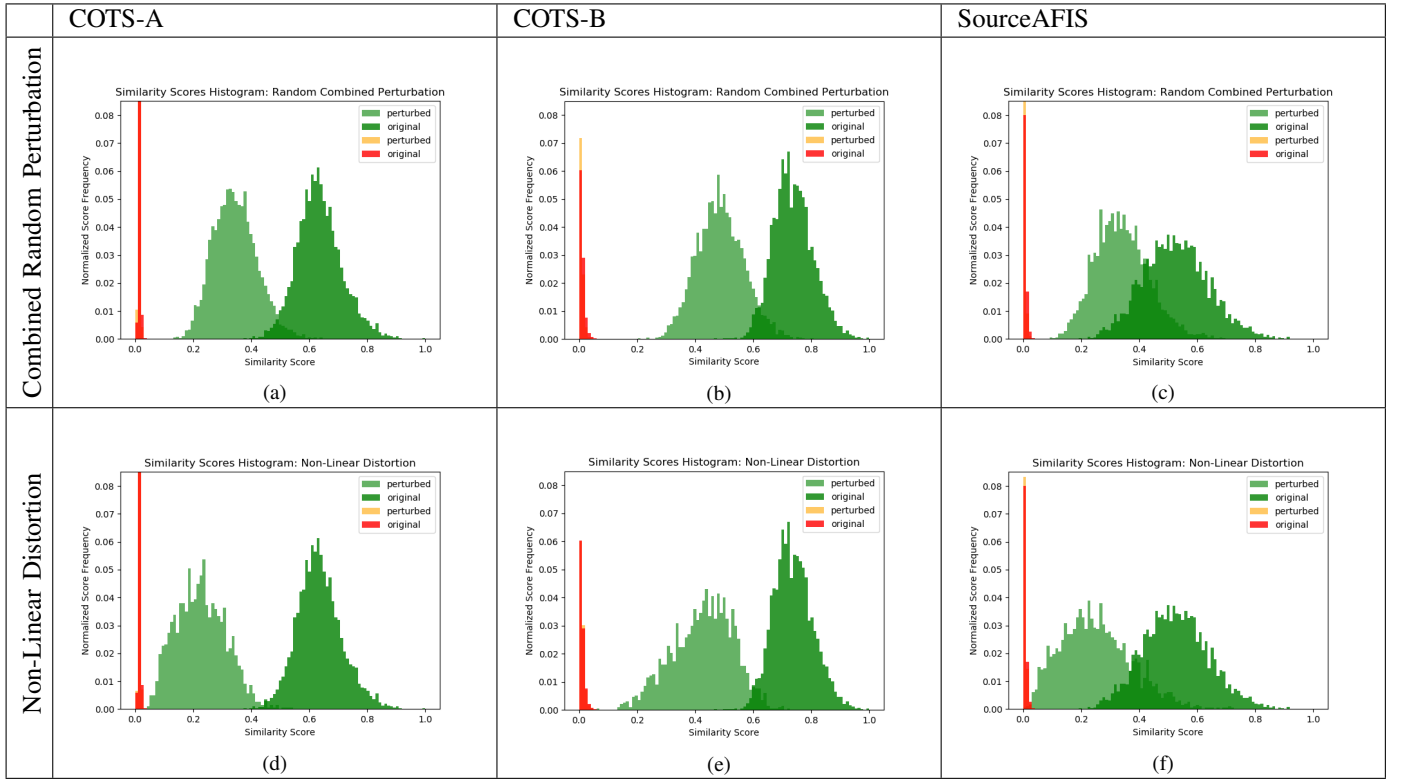


Fig. 9: Comparison on the effects of the combined random perturbations (translation/rotation shifts, missing minutiae, and spurious minutiae) and non-linear distortion on the genuine and imposter similarity scores obtained from each minutiae matcher: COTS-A, COTS-B, and SourceAFIS. The green and light-green distributions are the unperturbed and perturbed genuine similarity scores, respectively. The red and orange distributions are the unperturbed and perturbed imposter scores (scaled by 0.1), respectively. The normalized mean and standard deviation of the genuine and imposter similarity scores of the combined random perturbation, non-linear distortion, and the other perturbation techniques are shown in Table II.

spurious minutiae perturbation techniques both individually and combined on one synthetic impression of each pair. For each perturbed synthetic impression, we denote the perturbed minutiae feature set as $S'_{k,2}$. Thus, genuine similarity scores following the applied perturbations are computed between $S_{k,1}$ and $S'_{k,2}$ for each k .

Overall, we observe that the distribution of genuine scores following the random perturbations (position shifts, missing minutiae, spurious minutiae, and the combined model) differ significantly in comparison to the unperturbed distributions for each minutiae matcher. Notably, we see that the mean of

the perturbed genuine score distributions are all significantly lower in value than the mean of the unperturbed distributions. Among the random perturbations, the shift in the mean is most pronounced due to the combined perturbation. The effect of randomly removing minutiae is also prominent in decreasing the mean of the genuine similarity scores. However, the addition of spurious minutiae and the positional perturbations seemed to have little effect on the genuine scores. We expect these shifts in genuine similarity scores to degrade matcher accuracy. Lastly, we note that there is a minimal impact to the imposter score distributions. In fact, the only noticeable

shifts in the imposter distributions occurred in the spurious minutiae and combined random perturbation models. It is not surprising that the imposter scores are minimally impacted since minutiae-based matchers are fine-tuned for very low FAR, thus have very peaked imposter distributions centered near 0.

In general, we notice that the variance of the genuine similarity distributions following the random perturbations increases in all cases except for the SourceAFIS matcher, which experienced a slight decrease in variance due to the positional and spurious perturbation techniques. For each matcher, the largest increase in variance is seen with randomly removing minutiae, suggesting that the effect of missing minutiae has a more unpredictable and volatile impact on the performance of minutiae matchers. One explanation may be that certain minutiae contribute significantly more to the overall similarity score than others. Hence, the removal of such landmark points could drastically effect the similarity score produced by a minutiae matcher.

Analysis of the uncertainty scores for each matcher due to the various random perturbation techniques shown in Table III indicate that missing minutiae and the combined perturbation model generate the greatest measurement uncertainty. This agrees with the similarity score distributions where we see the largest increase in variance due to the missing and combined perturbations.

B. Effect of Non-Linear Distortion

(d), (e), and (f) of Figure 9 show the effects of the non-linear distortion. Out of all perturbation techniques in the study, the non-linear distortion has the greatest impact on decreasing the mean of the genuine similarity score and increasing the variance for each matcher. The non-linear distortion also produces the greatest measurement uncertainty for each matcher. Thus, it is evident that realistic levels of non-linear distortion have a tremendous effect on lowering the effectiveness of minutiae-based matchers. This is evidence for concern since it is commonly known that criminals will deliberately attempt to obscure their real identities by applying some non-linear distortion to their fingerprint impressions. This motivates further research into minutiae-based matchers or some other fingerprint matching algorithms that are more robust to non-linear distortion. Alternatively, algorithms for detecting and correcting for non-linear distortion should be developed and incorporated into minutiae-based matchers.

C. Recognition Accuracy vs. Amount of Perturbation

Figure 10 shows the TAR at a constant FAR of 0.01% for each minutiae matcher. In panel (c) of Figure 10, we observe that randomly adding spurious minutiae on its own has no effect on the recognition accuracy of the COTS minutiae-based matchers and very little effect for the SourceAFIS matcher until exceeding 200% spurious minutiae. Furthermore, increasing the positional perturbation and the number of missing minutiae has very little effect for all matchers up to a perturbation level at which the performance drops steeply. Panels (a) and (b) of Figure 10 indicate that these inflection points are at about 15

to 20 pixels for the positional displacement and around 80% to 85% for the percentage of missing ground truth minutiae. Panel (d) shows a similar sudden drop in recognition accuracy for the combined random perturbation around a combined 10 pixel displacement, 40% minutiae removal, and 100% minutiae addition. Interesting to note that individually, these levels of perturbation allow for greater than 95% accuracy, but when aggregated together produce near 0% accuracy. Finally, (e) shows that the effect on increasing amounts of non-linear distortion is more gradual, yet still detrimental to recognition accuracy.

Comparing the robustness of each matcher to the increasing perturbation, we see that the SourceAFIS matcher consistently shows greater recognition accuracy decline than either of the COTS matchers. The greater degradation in recognition performance for the SourceAFIS matcher is also more steep compared to the other two matchers. This suggests that the COTS minutiae based matchers are relatively more robust to the induced perturbations, however, we see that with enough random positional perturbations and non-linear distortion, these matchers also show significant performance decline.

IV. CONCLUSION AND FUTURE WORK

While past end-to-end evaluations such as FpVTE 2012 [8] have provided analysis of baseline statistics on state-of-the-art fingerprint recognition systems, work is still to be done on providing insight into the individual performance of sub-models within the larger system. To that end, we proposed a standardized evaluation protocol for white-box testing fingerprint minutiae-matchers. In particular, we have computed the measurement uncertainty of an open source minutiae matcher SourceAFIS, as well as two state-of-the-art commercially available matchers Innovetrics and Verifinger to various normally-distributed perturbations to their inputs (minutiae feature sets). Additionally, similarity score distributions between ground truth minutiae and perturbed minutiae were calculated to enable an extensive white-box evaluation on the robustness of minutiae-matchers to the introduced perturbations. Our results indicate that realistic random positional perturbation and non-linear distortion to input minutiae locations may drastically affect the similarity scores output by minutiae-based matchers.

It was determined that certain perturbation techniques had a conclusive effect on the similarity scores assigned by each matcher in the study. Concretely, it was found that non-linear distortion has the greatest effect of lowering the similarity scores between an unperturbed impression and a corresponding perturbed impression, whereas adding spurious minutiae had the least effect. Furthermore, the uncertainty analysis of genuine similarity scores between impressions after each perturbation determined that the non-linear distortion produced the greatest uncertainty in its genuine similarity scores and the least uncertainty was experienced with the translational and rotational perturbations. These findings suggest that minutiae-based matchers are relatively robust to slight positional and spurious minutiae perturbations, but weak to non-linear distortion and random removal of minutiae. Further study will be

TABLE II: Similarity Score Distribution Statistics of Various Perturbations

		Unperturbed	Positional	Missing	Spurious	Combined	Non-Linear Distortion
Genuine Avg.(s.d.)	COTS-A	0.636 (0.078)	0.498 (0.058)	0.494 (0.107)	0.557 (0.087)	0.345 (0.076)	0.227 (0.085)
	COTS-B	0.738 (0.068)	0.640 (0.064)	0.629 (0.090)	0.665 (0.077)	0.487 (0.081)	0.427 (0.104)
	SourceAFIS	0.527 (0.114)	0.481 (0.100)	0.391 (0.121)	0.473 (0.108)	0.341 (0.094)	0.253 (0.121)
Imposter Avg.(s.d.)	COTS-A	0.015 (0.004)	0.015 (0.004)	0.014 (0.004)	0.014 (0.004)	0.013 (0.004)	0.015 (0.008)
	COTS-B	0.010 (0.009)	0.009 (0.009)	0.010 (0.009)	0.008 (0.008)	0.007 (0.007)	0.010 (0.009)
	SourceAFIS	0.007 (0.006)	0.006 (0.006)	0.006 (0.005)	0.005 (0.005)	0.005 (0.005)	0.006 (0.005)

TABLE III: Uncertainty Scores of Various Perturbations

	Positional	Missing	Spurious	Combined	Non-Linear Distortion
COTS-A	0.0008	0.0094	0.0049	0.0060	0.0288
COTS-B	0.0011	0.0070	0.0046	0.0075	0.0249
SourceAFIS	0.0011	0.0046	0.0019	0.0073	0.0118



Fig. 10: True detect rate at a constant false detect rate of 0.01% of the three minutiae matchers vs. increasing levels of perturbation. (a) Increasing random minutiae position displacements (in pixels), (b) increasing percentage of ground truth minutiae removed, (c) increasing percentage of ground truth minutiae added, (d) increasing combined random noise (combined pixel displacements, missing minutiae, and spurious minutiae), and (e) increasing std. dev. values of the non-linear distortion model.

aimed at evaluating the effect of correlated noise to account for non-uniformity caused by the elasticity of human skin in positional displacement between the inner and outer edge of the fingerprint impressions.

Lastly, it was determined through an experiment on recognition performance vs. increasing levels of perturbations, that the effect of adding spurious minutiae on its own has very little effect on the accuracy of the minutiae-based matchers. Furthermore, a sharp decline in performance was experienced with the positional displacements, random removal of minutiae points, and the combined random noise perturbation models once a certain threshold of perturbation was reached. These thresholds were around 20 pixels for the positional displacement, 85% of

ground truth minutiae removed for the missing minutiae, and a combination of 10 pixels displacement, 40% missing minutiae, and 100% spurious minutiae for the combined model.

ACKNOWLEDGMENT

This research was supported by grant no. 70NANB17H027 from the NIST Measurement Science program. The views and conclusions contained herein are those of the authors and should not be interpreted as necessarily representing the official policies, either expressed or implied, of NIST, or the U.S. Government. The U.S. Government is authorized to reproduce and distribute reprints for governmental purposes notwithstanding any copyright annotation therein.

REFERENCES

- [1] D. Maltoni, D. Maio, A. K. Jain, and S. Prabhakar, *Handbook of Fingerprint Recognition*. Springer, 2nd ed., 2009.
- [2] S. S. Arora, K. Cao, A. K. Jain, and N. G. Paulter, "Design and fabrication of 3d fingerprint targets," *IEEE Transactions on Information Forensics and Security*, vol. 11, pp. 2284–2297, Oct. 2016.
- [3] S. S. Arora, A. K. Jain, and N. G. Paulter, "3d whole hand targets: Evaluating slap and contactless fingerprint readers," in *2016 International Conference of the Biometrics Special Interest Group (BIOSIG)*, pp. 1–8, Sept 2016.
- [4] S. S. Arora, A. K. Jain, and N. G. Paulter, "Gold fingers: 3d targets for evaluating capacitive readers," *IEEE Transactions on Information Forensics and Security*, pp. 1–1, Apr. 2017.
- [5] J. J. Engelsma, S. S. Arora, A. K. Jain, and N. G. Paulter, "Universal 3d wearable fingerprint targets: advancing fingerprint reader evaluations," *IEEE Transactions on Information Forensics and Security*, vol. 13, no. 6, pp. 1564–1578, 2018.
- [6] T. Chugh, S. S. Arora, A. K. Jain, and N. G. Paulter, "Benchmarking fingerprint minutiae extractors," in *2017 International Conference of the Biometrics Special Interest Group (BIOSIG)*, pp. 1–8, IEEE, 2017.
- [7] R. Black, *Managing the Testing Process: Practical Tools and Techniques for Managing Hardware and Software Testing*. Wiley Publishing, 3rd ed., 2009.
- [8] C. I. Watson, G. Fiumara, E. Tabassi, S. Cheng, P. Flanagan, and W. Salamon, "Fingerprint vendor technology evaluation, NIST Interagency/Internal Report 8034: 2015," available at <https://dx.doi.org/10.6028/NIST.IR.8034>.
- [9] "FVC2002," <http://bias.csr.unibo.it/fvc2002/>. 2002.
- [10] "FVC2004," <http://bias.csr.unibo.it/fvc2004/>. 2004.
- [11] "Improving Authentication Mechanisms for Enterprise." https://www.novetta.com/wp-content/uploads/2014/11/NOV_Biosynthetics_Overview-2.pdf.
- [12] B. T. Ulery, R. A. Hicklin, M. A. Roberts, and J. Buscaglia, "Measuring what latent fingerprint examiners consider sufficient information for individualization determinations," *PloS One*, vol. 9, no. 11, p. e110179, 2014.
- [13] B. T. Ulery, R. A. Hicklin, M. A. Roberts, and J. Buscaglia, "Changes in latent fingerprint examiners markup between analysis and comparison," *Forensic Science International*, vol. 247, pp. 54–61, 2015.
- [14] R. A. Hicklin, B. T. Ulery, T. A. Busey, M. A. Roberts, and J. Buscaglia, "Gaze behavior and cognitive states during fingerprint target group localization," *Cognitive Research: Principles and Implications*, vol. 4, no. 1, p. 12, 2019.
- [15] R. Cappelli, D. Maio, and D. Maltoni, "Sfinge: an approach to synthetic fingerprint generation," in *International Workshop on Biometric Technologies (BT2004)*, pp. 147–154, 2004.
- [16] R. Vazan, *SourceAFIS for Java and .NET*, (accessed June, 2019). <https://sourceafis.machinezoo.com>.
- [17] "Uncertainty analysis," *NIST/SEMATECH e-Handbook of Statistical Methods*, Jun 2003.
- [18] Y. Zhu, S. C. Dass, and A. K. Jain, "Statistical models for assessing the individuality of fingerprints," *IEEE Transactions on Information Forensics and Security*, vol. 2, no. 3, pp. 391–401, 2007.
- [19] E. Tabassi, "Towards NFIQ II Lite: Self-organizing maps for fingerprint image quality assessment," tech. rep., 2014.
- [20] X. Si, J. Feng, J. Zhou, and Y. Luo, "Detection and rectification of distorted fingerprints," *IEEE Transactions on Pattern Analysis and Machine Intelligence*, vol. 37, no. 3, pp. 555–568, 2015.
- [21] F. L. Bookstein, "Principal warps: Thin-plate splines and the decomposition of deformations," *IEEE Transactions on Pattern Analysis and Machine Intelligence*, vol. 11, no. 6, pp. 567–585, 1989.
- [22] "Evaluation of measurement data supplement 1 to the guide to the expression of uncertainty in measurement propagation of distributions using a monte carlo method," *JCGM 101*, 2008.



Joshua J. Engelsma graduated magna cum laude with a B.S. degree in computer science from Grand Valley State University, Allendale, Michigan, in 2016. He is currently working towards a PhD degree in the Department of Computer Science and Engineering at Michigan State University, East Lansing, Michigan. His research interests include pattern recognition, computer vision, and image processing with applications in biometrics. He won best paper award at ICB 2019 and is a student member of IEEE.



Nicholas G. Paulter Jr. is the Group Leader for the Security Technologies Group at NIST in Gaithersburg, MD. He develops and oversees metrology programs related to concealed weapon and contraband imaging and detection, biometrics for identification, and body armor characterization. He has authored or co-authored over 100 peer-reviewed technical articles and provided numerous presentations at a variety of technical conferences. He is a 2008-2009 Commerce Science and Technology Fellow and a 2010 IEEE Fellow.



Anil K. Jain is a University distinguished professor in the Department of Computer Science and Engineering at Michigan State University. His research interests include pattern recognition and biometric authentication. He served as the editor-in-chief of the IEEE Transactions on Pattern Analysis and Machine Intelligence. He is a member of the United States National Academy of Engineering and a Foreign Fellow of the Indian National Academy of Engineering.



Steven A. Grosz received his B.S. degree in electrical engineering from Michigan State University, East Lansing, Michigan, in 2019. He is beginning his PhD degree in the Department of Computer Science and Engineering at Michigan State University in the fall of 2019. His primary research interests are in the areas of machine learning and computer vision with applications in biometrics.